

Dislocation densities and lengths in solid ^4He from elasticity measurements

Ariel Haziot,¹ Andrew D. Fefferman,¹ John R. Beamish,^{1,2} and Sébastien Balibar¹

¹*Laboratoire de Physique Statistique de l'ENS, associé au CNRS et aux Universités Denis Diderot et P.M Curie, 24 rue Lhomond 75231 Paris Cedex 05, France*

²*Department of Physics, University of Alberta, Edmonton, Alberta, Canada T6G 2E1*

(Received 20 November 2012; revised manuscript received 5 January 2013; published 27 February 2013)

Measurements on solid ^4He show large softening of the shear modulus due to dislocations, behavior which has been described as giant plasticity. Dislocation networks may also be responsible for the unusual behavior seen in torsional oscillator and flow experiments. However, previous estimates of dislocation densities vary by many orders of magnitude, even in single crystals grown under similar conditions. By measuring the temperature and frequency dependencies of the elastic dissipation, we have determined dislocation densities and network lengths in ^4He single crystals, both in coexistence with liquid and at higher pressures, and in polycrystals grown at constant density. In all cases, dislocation lengths are much longer and the networks are less connected than previous estimates. Even in polycrystals, the dislocation network is far too sparse to explain the torsional oscillator results in terms of superfluidity in a dislocation network.

DOI: [10.1103/PhysRevB.87.060509](https://doi.org/10.1103/PhysRevB.87.060509)

PACS number(s): 67.80.bd, 61.72.Hh, 62.20.-x

Quantum effects are very important in solid helium and lead to unusual phenomena. The elastic properties of solid ^4He ¹⁻³ are strongly dependent on dislocations, which move freely in this quantum crystal. This can produce extremely large shear modulus changes described as “giant plasticity.”^{3,4} Torsional oscillator (TO) experiments on solid ^4He also show anomalous behavior below 200 mK,⁵ which has been taken as evidence of supersolidity. However, this interpretation has been challenged by recent calculations and experiments,⁶⁻¹⁰ which show that elastic effects in TOs are larger than previously assumed, suggesting that the anomalies may be elastic effects involving dislocations.

Annealing and plastic deformation^{2,11,12} affect both elastic and TO behaviors, confirming that dislocations are involved. At high temperatures, dislocations are strongly pinned at intersections but between these nodes they can move, which reduces the shear modulus. At low temperatures, ^3He impurities weakly pin them and restore the intrinsic stiffness. In a quantum solid, dislocations can have unique properties. Recent measurements on ^4He ⁴ showed that they can move freely in the basal plane, even at stresses as low as 10^{-9} bar. This extraordinary mobility may reflect delocalization of kinks; this would eliminate the Peierls barrier which limits dislocation motion in conventional crystals. Path integral Monte Carlo simulations,¹³ show that dislocations may have superfluid cores, which provides a possible mechanism for supersolidity¹⁴ and allows phenomena like superclimb.¹⁵ Recent experiments^{16,17} showed unusual flow, interpreted in terms of a Luttinger liquid in dislocation cores. The decoupling in a TO or the flux in a flow experiment depends on dislocation density Λ and on the network's connectedness. High-density networks have more intersections so the distance L between nodes is smaller. The combination ΛL^2 is a geometric parameter that characterizes the network's connectedness. In a simple cubic network $\Lambda L^2 = 3$, independent of dislocation density. Smaller values suggest additional pinning, while larger values imply that dislocations are aligned to avoid intersections.¹⁸

Despite their importance, and many experiments probing dislocation effects in helium, previous estimates of Λ vary

by six orders of magnitude. Some of this must reflect real differences arising from growth and deformation, but even in single crystals grown under similar conditions, reported densities vary by more than four orders of magnitude [$6 \times 10^9 \text{ cm}^{-2}$ (see Ref. 19) to $3 \times 10^5 \text{ cm}^{-2}$ (see Ref. 20)]. Even lower values, below 700 cm^{-2} , were found in crystals grown from the superfluid.²¹ X-ray topography²² has shown low-angle sub-boundaries in ^4He crystals, but individual dislocations could not be resolved so Λ and L could not be determined. The most detailed analyses applied the Granato-Lucke model²³ to ultrasonic measurements of sound speeds in single crystals grown from the normal liquid.²⁰ This treats dislocations as damped vibrating strings, driven by applied stress, and gave $\Lambda \approx 10^6 \text{ cm}^{-2}$ and $L \approx 5 \mu\text{m}$. The corresponding values of the network parameter ΛL^2 ranged from 0.1 to 0.2, but with a large uncertainty due to the unknown crystal orientations. However, nearly all TO experiments involved freezing at constant density. The large pressure changes and plastic deformation during such blocked capillary growth are expected to produce polycrystals with higher defect densities, but there have been no comparable ultrasonic measurements on such crystals and their dislocation densities are essentially unknown.

The effect of dislocations is simplest at low frequencies, where inertia and damping can be neglected. In this regime, the reduction of the shear modulus is proportional to ΛL^2 , but does not depend on Λ or L separately. A dislocation's contribution to strain is proportional to L^2 so a crystal with a few long dislocations can be softer than one with many short ones. The values of ΛL^2 inferred from low-frequency experiments are larger than those from ultrasonic measurements. TO shear modulus measurements at 331 Hz²⁴ gave $\Lambda L^2 \approx 2$ and recent measurements in the kilohertz range^{1,2} give similar values.

Although dislocation densities cannot be determined, even approximately, from the low-frequency shear modulus alone, the dissipation $1/Q$ provides additional information. A moving dislocation experiences a damping force B proportional to its speed v . Longer dislocations move faster and produce more dissipation. By measuring both modulus and dissipation, Λ and L can be separately determined, if B is known.

In contrast to previous estimates of L , which involved the frequency dependence²⁰ near the dislocations' resonance (around 12 MHz for $L = 5 \mu\text{m}$) or their breakaway from ^3He impurities,²⁵ we show directly that the dissipation at high temperatures is due to intrinsic dislocation damping from thermal phonons and use this dissipation to find L .

Our measurements were made in an optical cell, allowing us to determine crystal orientations from their growth facets.⁴ Single crystals were grown at temperatures as low as 20 mK, using either natural ^4He (nominal ^3He concentration 300 ppb) or isotopically pure ^4He (0.4 ppb ^3He). Two shear piezoelectric transducers (area $A = 1 \text{ cm}^2$) were mounted in the cell with a gap $D = 0.7 \text{ mm}$. An ac voltage V (between 200 Hz and 16 kHz) was applied to one transducer, generating a displacement $d_{15}V$ and a shear strain $\epsilon = \frac{Vd_{15}}{D}$ in the helium. The stress σ was determined from the current generated on the opposite transducer. The effective shear modulus $\mu = \frac{\sigma}{\epsilon}$ is given by a combination of the elastic constants C_{ij} which depends on the crystal's orientation.⁴ Dissipation was determined from the phase angle ϕ between stress and strain: $1/Q = \tan \phi$.

Figure 1 shows the (a) shear modulus and (b) dissipation at 3 kHz in crystal X21, grown from natural purity ^4He at 1.35 K. The modulus measured at low strain ($\epsilon = 10^{-9}$)

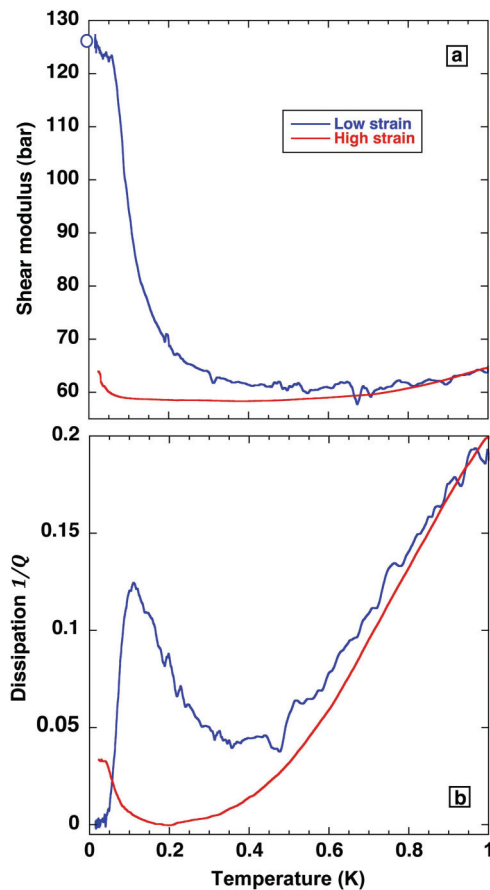


FIG. 1. (Color online) (a) Shear modulus and (b) dissipation measured at 3 kHz in a standard purity (300 ppb ^3He) crystal X21 grown at 1.35 K. Data are shown for two different strains, $\epsilon = 10^{-9}$ (noisy blue curves) and $\epsilon = 10^{-7}$ (red curves).

increases toward a “stiff” value at the lowest temperatures. We have shown⁴ that only C_{44} changes (as expected for dislocations gliding in the basal plane) and we calibrated the piezoelectric coefficient ($d_{15} = 0.95 \text{ \AA V}^{-1}$) using a crystal oriented so the shear modulus was nearly independent of C_{44} . The low-temperature modulus (126 bar) agrees with the value (the circle on the vertical axis) calculated from the orientation and the known elastic constants of helium.^{26–28} At higher temperatures, the modulus decreases by more than 50%. This softening, and the associated dissipation peak in Fig. 1(b), are due to unpinning of dislocations from ^3He impurities.¹ In the high-amplitude $\epsilon = 10^{-7}$ data, the effects of ^3He are almost eliminated since the large stress depins dislocations. The modulus in the soft state is nearly constant between 0.1 and 0.6 K.

Above 0.6 K, the impurity pinning is insignificant so the modulus and dissipation are independent of strain and the $1/Q$ reflects the dislocation damping caused by thermal phonons. These scatter from dislocations' static strain fields (anharmonicity, which gives a damping coefficient $B \propto T^5$) or from mobile dislocations (“fluttering,” which gives a larger $B \propto T^3$). A dependence $B \propto T^n$ has been inferred from previous experiments but with a range of values for the exponent n . Ultrasonic experiments^{20,29} did not extract n from direct fits but were consistent with values between 1.5 and 3. Internal friction experiments at 10 and at 78 kHz³⁰ gave n in ranges of 2.1 to 2.8 and 1.1 to 1.7, respectively. TO measurements at 331 Hz²⁴ did extract n directly from a fit to the dissipation but gave $n \approx 2$, rather than the expected T^3 dependence. Although the value of n was not clear, the magnitude of B in ultrasonic experiments²⁰ was close to that expected for fluttering.³¹

Our measurements provide a stringent test of the dissipation mechanism (since dislocations give $1/Q \propto \omega B$) and of whether the damping is due to fluttering (which predicts $B \propto T^3$). In Fig. 2(a), we plot the high-amplitude dissipation data from Fig. 1(b) as a function of T^2 , T^3 , and T^5 . It is clear that at low temperatures $1/Q \propto T^3$. Figure 2(b) shows dissipation at 1.5, 3, and 9 kHz for this crystal, plotted versus ωT^3 . At low temperatures, the data for the three frequencies collapse onto a single linear curve, demonstrating that $1/Q$ is proportional to ωT^3 .

The Granato-Lücke²³ model describes the elastic effects of dislocations. Our measurements are at frequencies well below their resonance (inversely proportional to their length and $\approx 60 \text{ kHz}$ for dislocations spanning the gap between transducers, $L \approx 1 \text{ mm}$). In this regime, the dislocation strain has a relaxation form with real and imaginary (dissipative) parts:

$$\frac{\epsilon_{\text{dis}}}{\epsilon_{\text{el}}} = R \Sigma \Lambda L^2 \frac{1 - i\omega\tau}{1 + (\omega\tau)^2}, \quad (1)$$

where R is an orientation factor ($0 \leq R \leq 0.5$) giving shear stress in the dislocations' glide direction, and $\Sigma = \frac{4(1-\nu)}{\pi^3} \approx 0.09$. The relaxation time is $\tau = \frac{BL^2}{\pi^2 C}$, where $C = \frac{2\mu_{\text{el}} b^2}{\pi(1-\nu)}$, b is the Burgers vector ($3.7 \times 10^{-10} \text{ m}$), and ν is Poisson's ratio.

The total strain is the sum of elastic and dislocation contributions, so dislocations reduce the intrinsic shear modulus μ_{el}

and introduce dissipation:

$$\frac{\mu_{\text{el}}}{\mu} = \frac{\epsilon_{\text{el}} + \epsilon_{\text{dis}}}{\epsilon_{\text{el}}} = 1 + R\Sigma\Lambda L^2 \frac{1 - i\omega\tau}{1 + (\omega\tau)^2}. \quad (2)$$

The maximum softening, at low temperatures where the dislocation damping is small ($\omega\tau \ll 1$), is

$$\frac{\Delta\mu}{\mu_{\text{el}}} = \frac{\mu_{\text{el}} - \mu}{\mu_{\text{el}}} = \frac{R\Sigma\Lambda L^2}{1 + R\Sigma\Lambda L^2}, \quad (3)$$

while the dissipation in this regime is

$$\frac{1}{Q} = \frac{\Delta\mu}{\mu_{\text{el}}}\omega\tau = \frac{\Delta\mu}{\mu_{\text{el}}}\omega \frac{BL^2}{\pi^2 C}. \quad (4)$$

The dislocation damping is expected to be dominated by fluttering, which gives³¹

$$B = \frac{14.4k_B^3}{\pi^2\hbar^2 c^3} T^3, \quad (5)$$

where c is the Debye sound speed. This expression predicts damping that agrees (within a factor of two) with values from ultrasonic measurements.²⁰ For crystals grown at low temperatures, it gives $B \approx 1.49 \times 10^{-8} T^3$ Pa s. The ωT^3 dissipation in Fig. 2(b) confirms that this is the dominant damping mechanism.

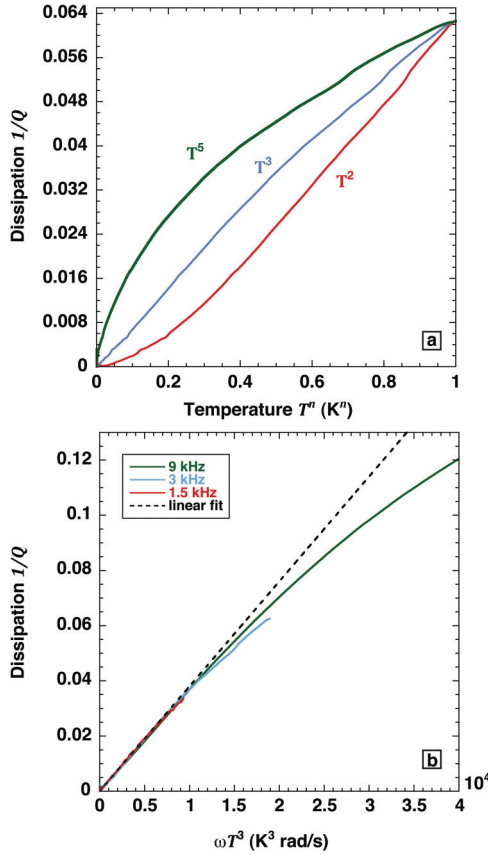


FIG. 2. (Color online) Dissipation at strain $\epsilon = 10^{-7}$, in an isotopically pure (0.4 ppb ^3He) crystal (X15c) grown at 1.37 K. (a) $1/Q$ at 3 kHz vs T^n for $n = 5$ (upper, green curve), $n = 3$ (middle, blue curve), and $n = 2$ (lower, red curve). (b) $1/Q$ at 1.5 kHz (red curve), 3 kHz (blue), and 9 kHz (green) vs ωT^3 . The dashed line is an extrapolation of the linear low- T behavior.

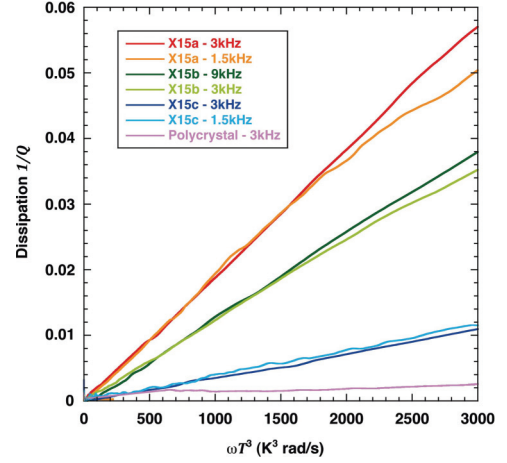


FIG. 3. (Color online) Dissipation at frequencies from 1.5 to 9 kHz in four different crystals, plotted vs ωT^3 .

At high temperatures and frequencies [e.g., for $\omega T^3 > 10^4$ in Fig. 2(b)], the dissipation deviates from this linear behavior because of the $(\omega\tau)^2$ term in the modulus [see Eq. (2)]. At higher temperatures, the dissipation will go through a maximum (for $\omega\tau \sim 1$) and then decrease as $\omega\tau$ increases. For $\omega\tau \gg 1$, dislocations are essentially immobile and do not contribute to dissipation or soften the crystal. This is why ultrasonic measurements made at high frequency and temperature give the intrinsic elastic constants of solid helium,^{26–28} unaffected by dislocations.

Figure 3 compares the dissipation for three types of crystals.⁴ The crystals grown at 0.60 and 0.02 K remained in coexistence with superfluid at all temperatures. The second type, grown above 1.3 K, solidified completely at higher pressure. The last type was a 29 bar polycrystal grown using the blocked capillary technique. Each has $1/Q \propto \omega T^3$ at low temperatures but the slopes vary, indicating different lengths L . We can calculate R from our known crystal orientations,⁴ Eqs. (3)–(5), and extract values of Λ and L from the modulus change $\Delta\mu/\mu_{\text{el}}$ and dissipation at low temperatures. Table I shows these values, and the network parameter ΛL^2 for crystals grown in the three ways described above, and from different purity ^4He .

Several assumptions affect our values of Λ and L . The value of C in Eq. (4) assumed isotropy and did not include the dislocation core energy. Equation (5) for the damping also assumes isotropy for phonon scattering but more precise calculations of C and B would not change the relative lengths in different crystals. We also assumed a single length L , with which we could reproduce the essential features of our

TABLE I. Dislocation parameters.

Crystal	T_f (K)	^3He (ppb)	L (μm)	Λ (cm^{-2})	ΛL^2
X15c	1.37	0.4	98	4.2×10^5	40.3
X18	1.32	0.4	98	5.9×10^5	56.6
X21	1.35	300	175	1.2×10^5	36.8
X15a	0.60	0.4	229	7.2×10^4	37.8
X15b	0.02	0.4	231	3.2×10^4	17.1
Polycrystal	(29 bar)	300	59	5.4×10^5	18.8

data. In the future, we will analyze the complete temperature and frequency dependence of both dissipation and modulus, including effects of a distribution of dislocation lengths. However, including a distribution will not drastically change the values of Λ and L , nor how they vary with crystal growth technique. Note that our measurements (like previous elastic and ultrasonic measurements) are sensitive only to mobile dislocations. Dislocations with glide planes in different directions may not be mobile; Λ and L in Table I refer only to dislocations that glide freely in helium's basal plane. Finally, the Granato-Lucke model is classical and does not consider possible dislocation damping due to zero point motion, which might be important when thermal damping can be neglected. It is difficult to measure absolute phase shifts needed to observe nonthermal damping, but we saw no evidence for significant damping at low temperatures.

The values of Λ in our single crystals are comparable to values previously inferred from some ultrasonic experiments,²⁰ suggesting that differences in cell geometry and growth technique do not dramatically change dislocation densities. However, network lengths L in our crystals are as much as 50 times longer. This may reflect the higher quality of single crystals grown from the superfluid at low temperatures, since our 20 mK crystals had the lowest Λ and those grown above 1.3 K had the highest. Our values of ΛL^2 (17 to 57) are much larger than expected for simple well-connected networks and at least two orders of magnitude larger than the ultrasonic values.^{20,21} These extremely large values indicate that dislocations are aligned in some way that minimizes intersections,⁴ probably in planar arrays¹⁸ like the low-angle grain boundaries observed in x-ray tomography.²²

The very large lengths also mean that dislocations vibrate with large displacements and velocities. For a strain

$\epsilon \sim 10^{-7}$, the maximum displacement of our longest dislocations ($L = 230 \mu\text{m}$) is $\xi_{\text{max}} = \frac{4\sigma b L^2}{\pi^3 C} \sim 1.5 \mu\text{m}$. The dislocation then sweeps out an area $\sim 4 \times 10^{-10} \text{ m}^2$ and would encounter about a thousand ^3He atoms in the natural purity crystals. However, the dissipation has the same ωT^3 dependence in the natural and isotopically pure crystals, so impurity scattering is not a significant source of dislocation damping at high temperatures. At a frequency of 9 kHz, $\xi_{\text{max}} = 1.5 \mu\text{m}$ corresponds to $v_{\text{max}} = \omega \xi_{\text{max}} \sim 0.1 \text{ m s}^{-1}$. This is significantly faster than the velocity of ballistically moving ^3He impurities ($v_3 \sim 2 \text{ mm s}^{-1}$) so it is possible that mobile ^3He cannot easily bind onto and pin such rapidly moving dislocations.

The blocked capillary polycrystal grown had higher dislocation densities and shorter lengths than single crystals, as expected, but the range of Λ is small compared to previous estimates. In the polycrystal, $\Lambda \sim 5.4 \times 10^5 \text{ cm}^{-2}$, only an order of magnitude larger than in the highest quality single crystals. At this density, less than one atom in 10^9 reside in the dislocation cores.

Our measurements have confirmed that the damping of dislocations in solid helium is dominated by scattering of thermal phonons, which produces a dissipation proportional to T^3 at low temperatures. This allowed us to extract consistent values of dislocation densities and lengths in single crystals and polycrystals. The densities are far smaller than the largest values sometimes quoted for solid helium ($6 \times 10^9 \text{ cm}^{-2}$),¹⁹ which essentially rules out the flow along the superfluid cores of a network of dislocations as the source of the apparent decoupling in torsional oscillator measurements.

This work was supported by grant ERC-AdG 247258 SUPERSOLID and by a grant from NSERC Canada.

¹J. Day and J. Beamish, *Nature (London)* **450**, 853 (2007).

²J. Day, O. Syshchenko, and J. Beamish, *Phys. Rev. B* **79**, 214524 (2009).

³X. Rojas, A. Haziot, V. Babst, S. Balibar, and H. J. Maris, *Phys. Rev. Lett.* **105**, 145302 (2010).

⁴A. Haziot, X. Rojas, A. D. Fefferman, J. R. Beamish, and S. Balibar, *Phys. Rev. Lett.* **110**, 035301 (2013).

⁵E. Kim and M. H. W. Chan, *Science* **305**, 1941 (2004).

⁶J. Beamish, A. Haziot, X. Rojas, A. Fefferman, and S. Balibar, *Phys. Rev. B* **85**, 180501 (2012).

⁷H. Maris, *Phys. Rev. B* **86**, 020502 (2012).

⁸X. Mi and J. Reppy, *Phys. Rev. Lett.* **108**, 225305 (2012).

⁹J. Reppy, X. Mi, A. Justin, and E. Mueller, *J. Low Temp. Phys.* **168**, 175 (2012).

¹⁰D. Y. Kim and M. H. W. Chan, *Phys. Rev. Lett.* **109**, 155301 (2012).

¹¹A. S. C. Rittner and J. D. Reppy, *Phys. Rev. Lett.* **98**, 175302 (2007).

¹²J. Reppy, *Phys. Rev. Lett.* **104**, 225301 (2010).

¹³M. Boninsegni, A. Kuklov, L. Pollet, N. Prokof'ev, B. Svistunov, and M. Troyer, *Phys. Rev. Lett.* **99**, 035301 (2007).

¹⁴S. Shevchenko, *Sov. J. Low Temp. Phys.* **14**, 553 (1988).

¹⁵S. Soyler, A. Kuklov, Pollet, N. Prokof'ev, and B. Svistunov, *Phys. Rev. Lett.* **103**, 175301 (2009).

¹⁶M. W. Ray and R. W. Hallock, *Phys. Rev. B* **79**, 224302 (2009).

¹⁷Y. Vekhov and R. W. Hallock, *Phys. Rev. Lett.* **109**, 045303 (2012).

¹⁸E. Varoquaux, *Phys. Rev. B* **86**, 064524 (2012).

¹⁹F. Tsuruoka and Y. Hiki, *Phys. Rev. B* **20**, 2702 (1979).

²⁰I. Iwasa, K. Araki, and H. Suzuki, *J. Phys. Soc. Jpn.* **46**, 1119 (1979).

²¹G. Lengua and J. Goodkind, *J. Low Temp. Phys.* **79**, 251 (1990).

²²I. Iwasa, H. Suzuki, T. Suzuki, T. Nakajima, H. Yonenaga, H. Suzuki, H. Koizumi, Y. Nishio, and J. Ota, *J. Low Temp. Phys.* **100**, 147 (1987).

²³A. Granato and K. Lucke, *J. Appl. Phys.* **27**, 583 (1956).

²⁴M. A. Paalanen, D. J. Bishop, and H. W. Dail, *Phys. Rev. Lett.* **46**, 664 (1981).

²⁵I. Iwasa, *J. Low Temp. Phys.* **171**, 30 (2013).

²⁶R. Crepeau, O. Heybey, D. Lee, and S. Strauss, *Phys. Rev. A* **3**, 1162 (1971).

²⁷D. Greywall, *Phys. Rev. B* **13**, 1056 (1971).

²⁸D. Greywall, *Phys. Rev. B* **16**, 5127 (1977).

²⁹R. Wanner, I. Iwasa, and S. Wales, *Solid State Comm.* **18**, 853 (1976).

³⁰V. Tsymbalenko, *Sov. Phys. JETP* **49**, 859 (1979).

³¹T. Ninomiya, *J. Phys. Soc. Jpn.* **36**, 399 (1974).